BEHAVIOR OF SLOPED-BOTTOM TUNED LIQUID DAMPERS

By S. Gardarsson,[1] Harry Yeh,[2] and Dorothy Reed,[3] Member, ASCE

ABSTRACT: The performance of a tuned liquid damper (TLD) with a sloped bottom of an angle of 30° with the horizontal is investigated experimentally. The sloped-bottom TLD was found to be just as effective in dissipating energy as the familiar box-shaped TLD. While the liquid motion of a box-shaped TLD resembles that of a hardening spring, the behavior of the sloped-bottom TLD resembles that of a softening spring. These different behaviors are due to different nonlinear effects: the amplitude dispersion effect and the wave runup effect onto the sloped surface, respectively. The sloshing force created by the motion of the sloped-bottom TLD was found in limited shaking table experiments to be comparable with that created by the equivalent box-shaped TLD, even though the net fluid mass of the sloped-bottom TLD is less than one half that of the box-shaped TLD. This behavior appears to be caused by the greater effective liquid mass involved in the sloshing motion in the sloped-bottom TLD.

INTRODUCTION

Tuned liquid dampers (TLD) are a structural vibration control device. They are comprised of liquid filled tanks whose sloshing motion is tuned to the natural frequency of the structure. Tuned liquid dampers are often placed at the top of the structure, and the liquid sloshing action counteracts and reduces the structural vibration. In practice, tuned liquid dampers are often made in circular, annular, and rectangular shapes, with the horizontal bottom dimension much greater than the liquid depth, so as to generate sufficient lateral forces with minimum liquid mass. Tuned liquid dampers of a rectangular shape with a flat horizontal bottom, i.e., box-shaped TLDs, have been investigated by many researchers (Fujino et al. 1988, 1990, 1992; Sun et al. 1989; Zhao and Fujino 1993; Koh et al. 1994; Gardarsson 1997; Reed et al. 1998; Yalla and Kareem 1999). It is well known that the nonlinear response of a box-shaped TLD resembles that of a hardening spring (Lepelletier and Raichlen 1988; Gardarsson 1997). In other words, the maximum response occurs at a frequency higher than that estimated by the linearized water-wave theory. One consequence of this characteristic is that the TLD is robust in dissipating energy over a wide frequency range (Reed et al. 1998). When force excitation occurs, water-wave motion in a TLD is established quickly in one or two sloshing periods. On the other hand, the established wave motion does not diminish immediately after the cessation of the excitation; i.e., there is some time lag for the liquid, usually water, to stop moving. This behavior of continual wave motion often causes the phenomenon of *beating* (amplitude modulation) during free oscillation (Chaiseri et al. 1989), which is clearly an adverse effect of the TLDs. The beating phenomenon is considered to be caused by a fraction of the energy absorbed by the TLD being transferred back to the structure, other than dissipating within the TLD (Fujino et al. 1988).

In order to mitigate this undesirable behavior, several attempts have been made to modify TLDs by increasing dissipation so as to stop the wave motion quickly after the cessation of forced excitation. The behavior of fluids that are more viscous than water was examined by Fujino et al. (1988, 1990). Fujino et al. (1988) also examined the influence of enhanced bottom roughness. Solid floats were placed in the water by Tamura et al. (1992) and, further, the effects of screens on energy dissipation were investigated by Zhao and Fujino (1993).

Effective wave-energy dissipation was the writers' initial motivation to investigate the performance of TLDs with the sloped bottom. It is well known that a sloping beach is an effective wave-energy dissipater. For example, to minimize wave reflection in a laboratory wave tank, an effective method is to install a sloping beach at the tank end wall. It is also well known that the majority of ocean waves are dissipated along the shores, especially due to wave breaking. Other anticipated features associated with the sloped-bottom tank are that, since the runup-height amplification is greater for the sloping beach than the vertical wall, wave motion in the TLD becomes more nonlinear than in the case of a box-shaped TLD, and a greater horizontal force might be created with less water mass. Note that, based on the fully nonlinear shallow-water-wave theory, the runup height R (the vertical distance from the still water level) for nonbreaking waves can be found to be

$$R = H\sqrt{\frac{\pi}{2\alpha}} \tag{1}$$

where H = offshore incident wave height, and α = beach slope in radians from horizontal (e.g., Mei 1983). Hence, the more gentle the beach slope is, the higher the runup.

In this paper, the sloshing characteristics associated with a sloped-bottom TLD are discussed and compared with those for a box-shaped TLD. The fundamental dynamic behaviors associated with the sloshing motions are identified. Based on the identified characteristics, the advantages and disadvantages of a sloped-bottom TLD are discussed.

EXPERIMENTS

The experiments were performed on the precision shaking table facility at the University of Southern California. Fig. 1 depicts the general setup of the experiments. The shaking table has a 1.2 × 1.2 m platform which moves in a single horizontal direction with the hydraulic-servo system. The platform, of total weight 350 kg, is anchored onto the concrete floor. The table was designed and constructed for general structural testing, which usually involves much greater specimen masses than the TLD models used in the present experiments. Hence, overloading was not a consideration. A Plexiglas model TLD was mounted on a load cell, which was bolted directly onto the shaking table. For comparisons, the writers used a box-shaped tank that has the identical outer dimensions (59 cm long, 33.5 cm wide, 30 cm high), i.e., the tank shown in Fig.

[1]Formerly, Grad. Student, Dept. of Civ. and Envir. Engrg., Univ. of Washington, Seattle, WA 98195.

[2]Prof., Dept. of Civ. and Envir. Engrg., Univ. of Washington, Seattle, WA.

[3]Prof., Dept. of Civ. and Envir. Engrg., Univ. of Washington, Seattle, WA.

Note. Associate Editor: James Beck. Discussion open until August 1, 2001. To extend the closing date one month, a written request must be filed with the ASCE Manager of Journals. The manuscript for this paper was submitted for review and possible publication on July 23, 1999; revised September 18, 2000. This paper is part of the ***Journal of Engineering Mechanics***, Vol. 127, No. 3, March, 2001. ©ASCE, ISSN 0733-9399/01/0003-0266–0271/$8.00 + $.50 per page. Paper No. 21493.

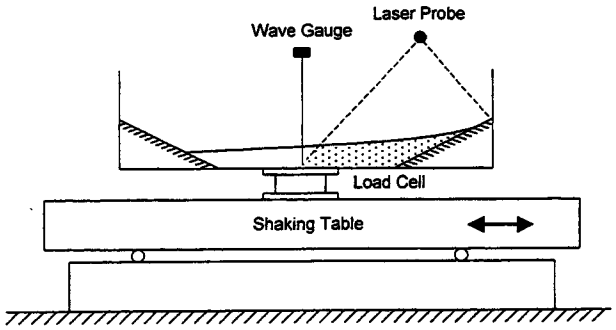

FIG. 1. Schematic View of Experimental Setup

1 but without the sloped bottom plates. The model TLDs are made of 1.27 cm thick Plexiglas plates with the bottom plate being 1.9 cm thick to ensure sufficient rigidity. For the sloped bottom TLD, the bottom slope was set to be 30° and the horizontal bottom bed is 9 cm long; no other cases with different slopes were examined. No special treatment was made to the Plexiglas, so the surface can be considered hydraulically smooth. Water was used as the liquid in all cases.

The wave response was measured with the capacitance-type wave gauges. The gauge itself is made of a Tantalum rod (0.5 mm in diameter) with an oxidized surface, which acts as dielectric for this capacitance-type wave gauge. The uniform tantalum oxide coating was achieved by anodizing the Tantalum rod in weak citric acid solution; the original idea of the use of a Tantalum rod for a capacitance gauge was provided by Chapman and Monardo (1991). The gauge was proven to be stable and precise; see Yeh and Chang (1994) for detailed description of the gauge.

In order to examine temporal and spatial variations of water-surface response, the laser-induced fluorescent imagery technique was used. In this technique, a 4-W Argon-ion laser beam is converted to a thin laser sheet by using a resonant scanner. With the aid of fluorescein dye dissolved in water, the vertical laser-sheet illumination from above induces the dyed water fluorescent and identifies a water-surface profile as well as a gradient of the water surface directly and nonintrusively. The illuminated images were recorded by video camera. A fast shutter speed, 1/250 s, was used to freeze the fast moving wave actions. The captured images were processed including the correction for image distortions; hence, the resulting images can be analyzed quantitatively. Detailed descriptions of the image process and the experimental setup can be found in Gardarsson (1997).

Before presenting our experimental results, the writers introduce the fundamental natural frequency of the water sloshing motion based on the linearized water-wave theory. For a box-shaped TLD, the dispersion relation yields

$$f_0 = \frac{1}{2}\sqrt{\frac{g}{\pi L}\tanh\frac{\pi h_0}{L}} \tag{2}$$

where f_0 = frequency in Hertz; g = acceleration of gravity; h_0 = water depth at rest; and for the lowest mode response, L = tank length. On the other hand, it is not simple to evaluate the dispersion relation for the sloped-bottom TLD shown in Fig. 1, because two different bottom slopes (horizontal and 30°) are involved. Nonetheless, the fundamental natural frequency can be inferred from one of the harbor-resonance solutions derived by Zelt (1986). The lowest-mode resonant condition for the geometry where a uniformly sloping plate connected with a uniform depth h_0 can be found to be

$$J_0(2\chi s)\cos\chi(1-s) = J_1(2\chi s)\sin\chi(1-s) \tag{3}$$

where J_0 and J_1 = Bessel functions of the first kind of order zero and one, respectively, and χ = nondimensionalized resonant frequency

$$\chi = \frac{\pi f W}{\sqrt{g h_0}} = \frac{\pi}{2}\frac{f_0}{f_{b0}}, \tag{4}$$

in which f_0 = resonant wave frequency, and f_{b0} = resonant wave frequency for a box-shaped tank [i.e., $T_{b0} = (1/f_{b0}) = (2W/\sqrt{gh_0})$ is the resonant wave period based on (2) for the shallow-water limit]. The parameter W = length of the still-water surface ($W = L$ for a box shaped tank); and s = geometric parameter that represents the ratio of the horizontal distance over the sloped surface to the entire water surface, i.e., $s = 0$ for a box-shaped tank and $s = 1$ for a triangular shaped tank. Based on (3) and (4), the relation between f_0/f_{b0} and s is plotted in Fig. 2 to find the fundamental resonant frequency for the sloped bottom tank.

RESULTS

In order to describe the characteristics and behavior of the sloped bottom TLD, the writers examine the experimental results with water depth $h_0 = 4.0$ cm and excitation amplitude $A = 5$ mm. The net fluid mass is 2.28 kg. With this water depth ($h_0 = 4.0$ cm) and the length of the still-water surface $W = 22.86$ cm, the value of the geometric parameter s in (3) is $s = 0.606$ (=13.86/22.86 cm). Then, Fig. 2, or alternatively (3) and (4), yields the fundamental natural frequency of the sloshing $f_0 = 1.258$ Hz.

For the quantitative comparison, the writers also examine the box-shaped TLD with the water depth $h_0 = 3.0$ cm, the natural sloshing frequency $f_0 = 0.458$ Hz based on (2), and the excitation amplitude $A = 40$ mm. For these parameters, the excitations applied to both TLDs are comparable; i.e., the maximum excitation acceleration at the natural sloshing frequency f_0 for the sloped-bottom TLD is 32.4 cm/s^2, while the acceleration for the box-shaped TLD is 33.1 cm/s^2. However, it is noted that the net fluid mass of the box-shaped TLD is 5.93 kg, which is more than 2.5 times that of the sloped-bottom TLD.

Temporal and spatial variations of the water surface profiles along the centerline of both the box-shaped and sloped-bottom tanks for their maximum response are shown in Fig. 3. Each wave profile was captured by the laser-induced fluorescent image technique with the vertical laser light sheet along the tank centerline and the captured images were corrected for distor-

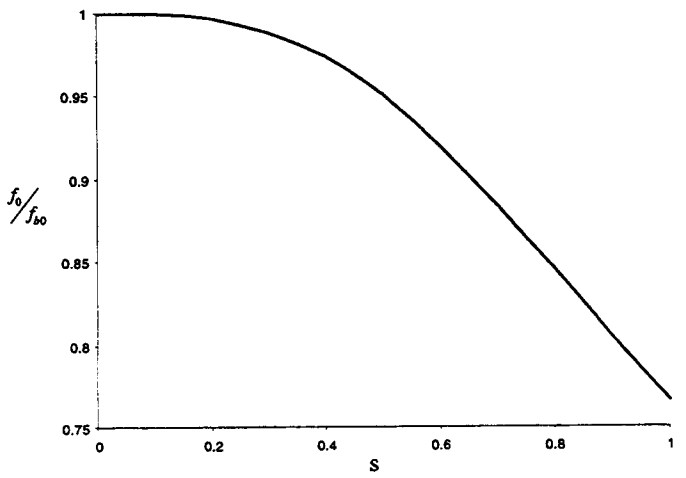

FIG. 2. Resonant Wave Frequency, f_0, for Sloped-Bottom TLD, Normalized by Resonant Frequency, f_{b0}, for Box-Shaped TLD, Based on Eqs. (3) and (4) (Frequency Is a Function of Shape Parameter s, Where s = Ratio of Horizontal Distance over Sloped Surface to Entire Water Surface)

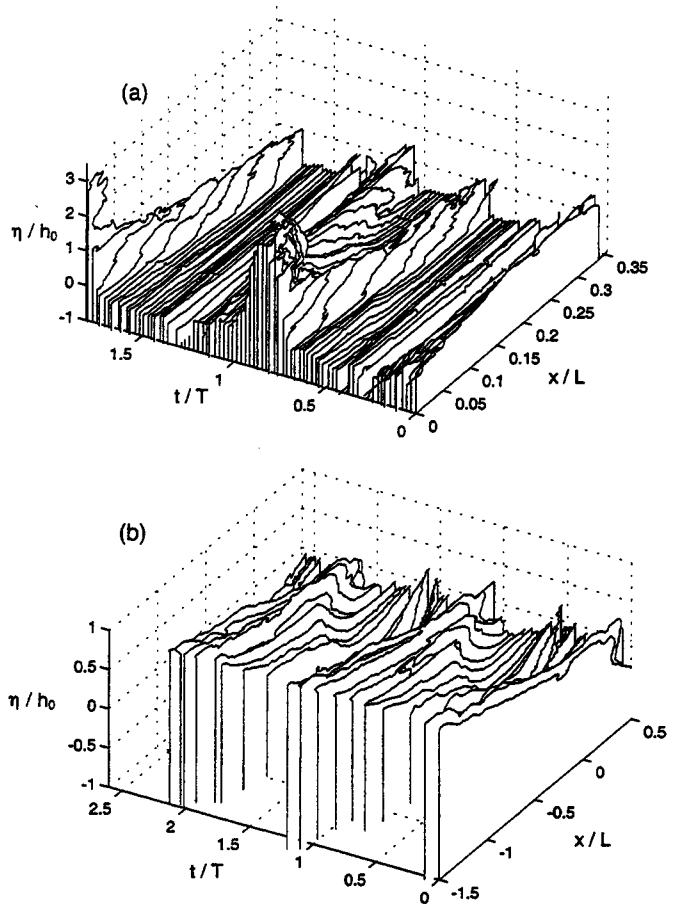

FIG. 3. Temporal Variations of Water-Surface Profiles When Response Is Maximum: (a) Box-Shaped TLD at β = 1.50; (b) Sloped-Bottom TLD at β = 0.91 (Toe of Sloped Bottom Is at *x/L* = 0)

tion. The processed spatial water-surface profile images, which are 30 frames per second, were stacked together to represent the temporal variations. In the figures, the time t is normalized by the excitation period T (=$1/f_0$), the water surface elevation η from the still-water level is normalized by the still-water depth h_0, and x is the longitudinal distance along the tank center line with the origin located at the end wall for the box-shaped TLD [Fig. 3(a)] and at the slope toe for the sloped-bottom TLD [Fig. 3(b)]. The longitudinal distance x was normalized by the horizontal bed length, i.e., the distance between the beach toes. The water-surface profiles of one-half of the tank length are presented in Fig. 3. Because the tank is symmetric and the imposed excitation is purely oscillatory, the water-surface variations in the other half of the tank should be identical to those shown in the figures except that the phase is shifted by π. Also note that the excitation frequency f is normalized by the fundamental natural frequency f_0 predicted from the linearized wave theory, i.e., (2) and (3), such that the ratio $\beta = f/f_0$. It is noted that the maximum response of the sloped-bottom tank occus at $\beta = 0.91$, whereas that of the box-shaped tank occurs at $\beta = 1.50$. The implications of this finding will be discussed in detail later on.

As shown in Fig. 3, there are more stacked profiles for the box-shaped TLD because its excitation frequency is smaller; hence, more profile data are generated per each oscillation. Fig. 3(a) shows that there is a strong bore that strikes and reflects at the end wall, and the maximum splash-up tip at the end wall could not be measured because its height was outside of the range for the video camera. Some of the profiles in both Figs. 3(a and b) exhibit clear wave breaking with the overturning water surface, but the wave patterns shown in Fig. 3(b) are much more complex than those in Fig. 3(a). Note that these complex waves appear to have short wave lengths and such features do not significantly affect the primary sloshing motion.

Temporal variations of the (vertical) runup elevations for both the sloped-bottom and box-shaped TLDs at the maximum response are shown in dimensional form in Fig. 4. The runup data were extracted from the (calibrated) video images, such as shown in Fig. 3. In Fig. 5, the corresponding water-surface variations at the midtank location $x/L = 0.5$ are plotted. It can be seen in Fig. 4 that the runup (vertical) height along the sloping plate (the difference between the maximum and minimum) is comparable to that of the box-shaped tank at the end wall. However, there is a distinct difference in the runup profiles. The wave crests in the sloped-bottom tank have a prolonged broad shape, whereas the waves in the box-shaped tank can be characterized as the short pulse formations. The wave height at the center of the sloped-bottom tank, as shown in Fig. 5, is much smaller than, approximately one-fifth, that in the box-shaped tank. If the response were small and the wave motion were linear, then the node of the standing wave would have been formed at the midsection of the tanks and no water-surface fluctuation should have occurred at the node. The large fluctuation for the box-shaped TLD as shown in Fig. 5 results from the fact that, when the TLD responds significantly, the sloshing motion in the tank is that of the back-and-forth bore (broken waves) formation, as seen in Fig. 3(a), in which the resulting water-surface fluctuations are large. Note that the back-and-forth bore formations manifest themselves as sawtooth temporal profiles appearing in Fig. 5.

Also apparent in Fig. 5 is the significant reduction of mean water level at the center of the sloped-bottom tank during the large response. The mean water level at the midpoint is $\bar{\eta} = -8$ mm or $\bar{\eta}/h_0 = -0.2$, in the sloped-bottom tank, while $\bar{\eta} \approx 0$ in the box-shaped tank. Fig. 6 presents examples of minimal, peak, and reduced peak wave motion at the midpoint of the sloped-bottom tank. As mentioned previously, the maximum excitation, in terms of water-surface oscillations, in the sloped-bottom tank takes place at the excitation frequency $\beta = 0.91$, while that in the box-shape tank takes place at $\beta = 1.50$. Further, the variation in the set-down for the sloped-bottom tank

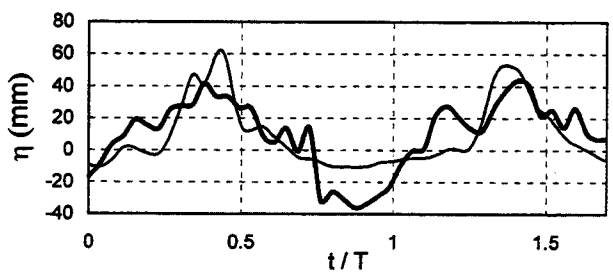

FIG. 4. Temporal Variations of Water-Surface Elevations at End of Tank: Bold Line = Sloped-Bottom Tank at β = 0.91; Thin Line = Box-Shaped Tank at β = 1.50

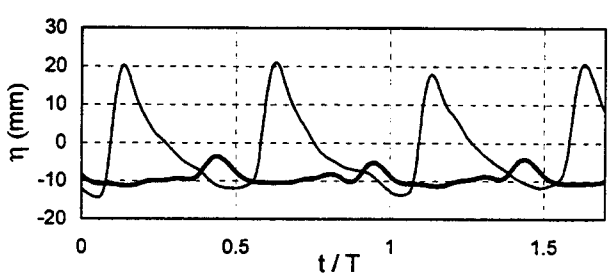

FIG. 5. Temporal Variations of Water-Surface Elevations at Middle of Tank: Bold Line = Sloped-Bottom Tank at β = 0.91; Thin Line = Box-Shaped Tank at β = 1.50

does not occur when the tank response is relatively small, as shown in Fig. 6, where the wave gauge data of the water-surface variations at the midpoint are presented. As previously stated, when the response is small, the wave action is a simple back-and-forth sway motion. In this case, the center of the tank becomes the node of the swaying standing wave formation without the set-down effect. Once the response builds up to a significant sloshing, the water motion becomes a back-and-forth "flow" with the wave breaking on the beach. The sloshing behaviors are schematically characterized in Fig. 7. As the response builds, the entire water mass shifts back-and-forth with a substantial depression in water level at the center of the tank. Hence, the effective mass of the TLD increases significantly. No such behavior was detected for the box-shaped tank; the back-and-forth bore propagation is formed instead.

As described by Lepelletier and Raichlen (1988) and Gardarsson (1997), box-shaped TLDs possess a hardening spring property. As excitation frequency increases, the TLD response increases until a certain limit at the "jump frequency." Beyond the jump frequency, the response suddenly ceases; i.e., a quenching phenomenon occurs in this region. All empirical

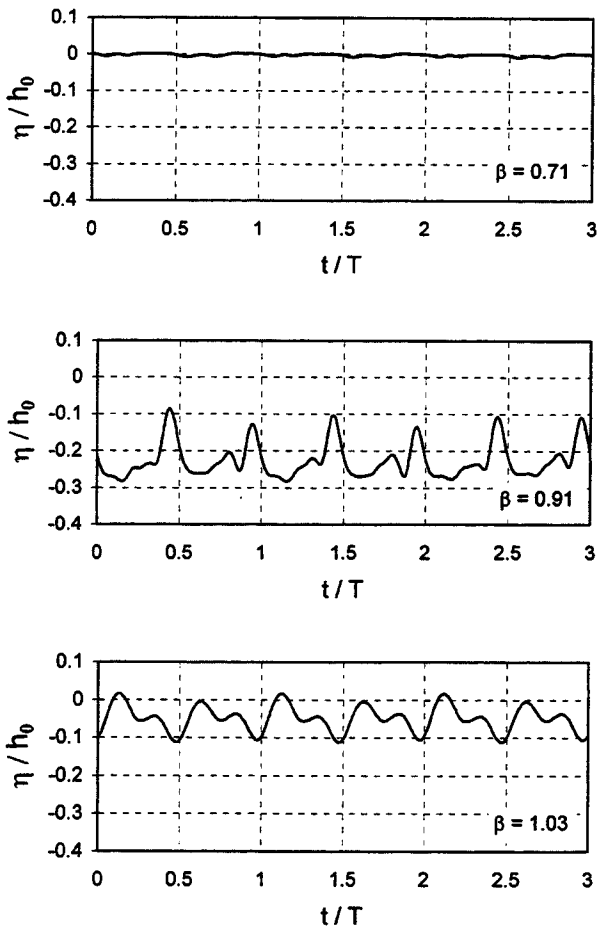

FIG. 6. Temporal Variations of Water-Surface Elevations at Middle of Sloped-Bottom Tank

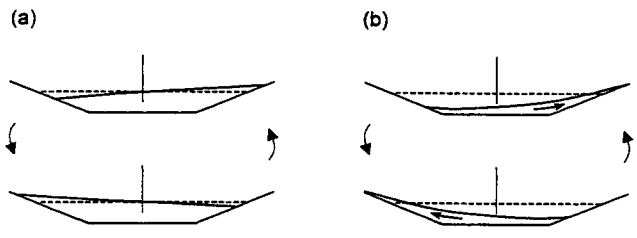

FIG. 7. Sketches of Sloshing Patterns: (a) Small Response; (b) Large Response

data for this sloped-bottom tank display a softening spring behavior; that is, the maximum excitation (and jump phenomenon) occurs at a frequency ratio less than unity ($\beta = 0.91 < 1.0$). The implications are as follows: (1) tuning of the sloped-bottom tank for maximum damping involves matching its linear natural frequency to a value slightly higher than the structure's fundamental frequency; and (2) buildings with a tendency to undergo significant stiffness degradation during strong motion excitation might benefit from the softening behavior provided by the sloped tank. That is, the tank will not be "dynamically mistuned" as the impact of the excitation is felt. Another positive aspect of the sloped tank, as illustrated in Fig. 7, is the effective use of the liquid mass. It has been estimated that only a small portion of the liquid mass fully participates in the control process for box-shaped tanks; these new results suggest that the sloped-bottom tank makes better use of the entire mass.

If the tank with a 30° sloped side exhibits softening behavior, and the box exhibits hardening behavior, then perhaps at some angle in between 0 and 30°, the sloshing will exhibit "stiffness-neutral" behavior; that is, the peak wave motion will occur at the linear tuned frequency. The implications of this property are not clear at this time but remain open for further investigation.

In addition to the tuning aspects, the estimation of the maximum sloshing force, often termed the "base shear," in structural control applications is essential. The base-shear forces caused by the sloshing actions were obtained by subtracting the inertial forces of the empty container by itself from the forces measured with the load cell (see Fig. 1). The response forces for both box-shaped and sloped-bottom TLDs are plotted for a range of excitation frequencies in Fig. 8. The maximum response of the sloped-bottom tank is comparable to that of the box-shaped tank, in spite of the fact that the net water mass of the sloped-bottom TLD is less than half that of the box-shaped TLD. Evidently, a much greater response force of the sloped-bottom TLD would result if the net water mass is adjusted as to be the same as that of the box-shaped TLD, for example, by installing multiple sloped-bottom TLDs.

Because exact dynamic similitude is not possible without satisfying the geometric similitude between box-shaped and sloped-bottom TLDs, another comparison is made and presented as a supplement to the result shown in Fig. 8. Instead of the maximum acceleration, the water mass and the excitation amplitude were matched for this comparison. The writers set the water depth $h_0 = 3$ cm and the excitation amplitude $A = 2.5$ mm for the box-shaped TLD. The resulting water mass for this TLD is 5.93 kg. For the sloped-bottom TLD, the case examined had $h_0 = 10$ cm deep water with a water mass of 4.67 kg, with the identical excitation amplitude. The resulting response forces are shown in Fig. 9, which clearly demonstrate

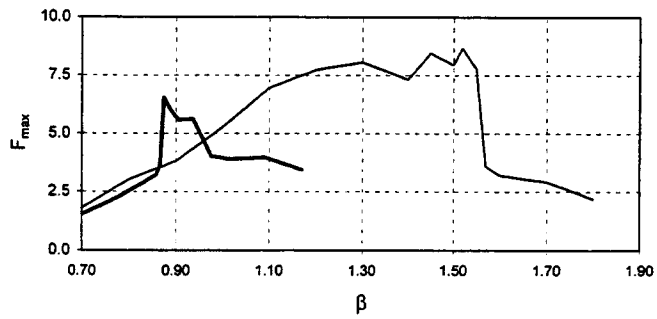

FIG. 8. Comparison of Base Shear Force in Newtons: Bold Line = Sloped-Bottom Tank; Thin Line = Box-Shaped Tank (To Match Applied Excitation in Terms of Acceleration, Writers Used $A = 40$ mm and $f_0 = 0.458$ Hz for Box-Shaped TLD, and $A = 5$ mm and $f_0 = 1.258$ Hz for Sloped-Bottom TLD)

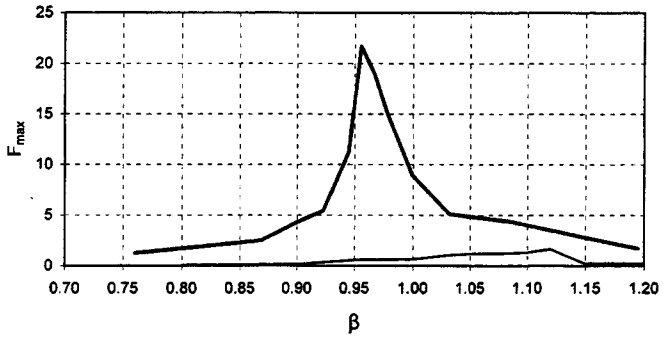

FIG. 9. Comparison of Base Shear Force in Newtons: Bold Line = Sloped-Bottom Tank; Thin Line = Box-Shaped Tank (To Match Water Mass and Excitation Amplitude, Writers Used A = 2.5 mm and h_0 = 3.0 cm for Box-Shaped TLD, and A = 2.5 mm and h_0 = 10.0 cm for Sloped-Bottom TLD

greater response force of the sloped-bottom TLD than that of the box-shaped TLD. It should be noted that, unlike the results in Fig. 8, the comparison in Fig. 9 does not represent the similar condition in terms of their dynamics acceleration (or their dynamic behavior).

The hardening-spring type behavior of the box-shaped TLD can be explained by the nonlinear effect on the wave propagation speed. Based on the nonlinear shallow-water wave theory, the propagation speed C of a uniform bore is

$$C = \sqrt{gh}\,\sqrt{\gamma\left(\frac{1+\gamma}{2}\right)} \tag{5}$$

where h = water depth ahead of the bore front and γ = ratio of the water depth of the bore to h. Since the value of γ is greater than unity, the propagation speed C increases as the bore height γ increases. This prediction is, of course, the ideal condition and cannot apply directly to the tank sloshing conditions considered here. Nonetheless, (5) clearly demonstrates that the nonlinear effect of the amplitude dispersion causes the increase in propagation speed. Hence, when the excitation frequency is higher than that of the linear resonance prediction, the corresponding wave motion in the tank becomes greater and in turn creates greater response forces. This explains the hardening-spring-type behavior of box-shaped TLDs.

On the other hand, the wave motion in the sloped-bottom tank involves the wave runup onto the sloping surface. Therefore, the larger the wave motion, the longer the runup will be, i.e., the effective tank length increases. Hence, the wave amplitude is greater at a frequency lower than that of the predicted value that is based on the linearized wave theory. Evidently, for the bottom slope of 30°, the nonlinear effect associated with the runup process is greater than the nonlinear effect of the amplitude dispersion. Consequently, the sloped-bottom TLD exhibits softening-spring-type dynamic behavior.

CONCLUSIONS

A box-shaped TLD behaves like a hardening spring, because of the nonlinear effect of amplitude dispersion. On the other hand, the sloped-bottom TLD examined in this study behaves like a softening spring, because of the nonlinear effect of the wave runup onto the sloped surface. The sloped-bottom TLD is especially effective when it is tuned slightly higher than the structure's fundamental response frequency.

Although direct quantitative comparisons between the box-shaped and the sloped-bottom TLDs are difficult for a given excitation for the damper (since individual parameters are different, such as the tuned frequencies, excitation amplitudes, and net fluid masses), the sloped-bottom TLD responds with a greater sloshing force than that of the equivalent box-shaped TLD with the same water mass. This increased energy dissipation occurs because, as demonstrated in the sketch in Fig. 7, a greater amount of water mass is placed into motion along the sloped bottom. In other words, the effective mass is greater than that of the box-shaped TLD.

While the sloped-bottom TLD appears to perform better than the box-shaped TLD, there are several factors that need to be considered for its practical implementation. Because of the sloped bottom, there will be a resulting greater magnitude of the moment exerted at the TLD base, which might cause installation problems. The performance of sloped-bottom TLDs with steeper angles should be investigated. Since a box-shaped TLD behaves like a hardening spring and the 30° sloped-bottom TLD behaves like a softening spring, there must be an angle at which neutral behavior occurs, although the benefits of such characteristics for tuned liquid dampers are uncertain. A similar variation can be expected if we lengthen the horizontal portion of the sloped-bottom TLD.

ACKNOWLEDGMENTS

The writers would like to acknowledge the assistance provided by Dr. J. Yu and Dr. T. Wakahara with our laboratory experiments. The writers would like to thank Dr. S. Masri for arranging the use of the shaking table facility at the University of Southern California. The support of the U.S. National Science Foundation (Grant No. CMS-9301577) for this project is gratefully acknowledged.

APPENDIX I. REFERENCES

Chaiseri, P., Fujino, Y., Pacheco, B. M., and Sun, L. M. (1989). "Interaction of tuned liquid damper (TLD) and structure—theory, experimental verification and application." *Struct. Engrs./Earthquake Engrg.*, Tokyo, 6, 273–282.

Chapman, R. D., and Monardo, F. M. (1991). "APL wave gage system." *Rep. No. SIR-91U-041*, Applied Physics Lab., Johns Hopkins University, Baltimore.

Fujino, Y., Pacheco, B. M., Chaiseri, P., and Sun, L.-M. (1988). "Parametric studies on tuned liquid damper (TLD) using circular containers by free-oscillation experiments." *Struct. Engrs./Earthquake Engrg.*, Tokyo, 5, 381–391.

Fujino, Y., Pacheco, B. M., Chaiseri, P., Sun, L.-M., and Koga, K. (1990). "Understanding of TLD properties based on TMD analogy." *J. Struct. Engrg.*, Tokyo, 36A, 577–590 (in Japanese).

Fujino, Y., Sun, L., Pacheco, B. M., and Chaiseri, P. (1992). "Tuned liquid damper (TLD) for suppressing horizontal motion of structures." *J. Engrg. Mech.*, ASCE, 118, 2017–2030.

Gardarsson, S. (1997). "Shallow-water sloshing." PhD thesis, University of Washington, Seattle.

Koh, C. G., Mahatma, S., and Wang, C. M. (1994). "Theoretical and experimental studies on rectangular liquid dampers under arbitrary excitations." *Earthquake Engrg. and Struct. Dyn.*, 2, 17–31.

Lepelletier, T. G., and Raichlen, F. (1988). "Nonlinear oscillations in rectangular tanks." *J. Engrg. Mech.*, ASCE, 114(1), 1–23.

Mei, C. C. (1983). *The applied dynamics of ocean surface waves*, Wiley, New York.

Reed, D., Yu, J., Yeh, H., and Gardarsson, S. (1998). "Investigation of tuned liquid dampers under large amplitude excitation." *J. Engrg. Mech.*, ASCE, 124(4), 405–413.

Sun, L. M., Fujino, Y., Pacheco, B. M., and Isobe, M. (1989). "Nonlinear waves and dynamic pressures in rectangular tuned liquid damper (TLD)—simulation and experimental verification." *Struct. Engrs./Earthquake Engrg.*, Tokyo, 6, 251–262.

Tamura, Y., Kousaka, R., and Modi, V. J. (1992). "Practical application of nutation damper for suppressing wind-induced vibrations of airport towers." *J. Wind Engrg. and Ind. Aerodyn.*, 41/44, 1919–1930.

Yalla, S., and Kareem, A. (1999). "Modelling tuned liquid dampers as sloshing-slamming dampers." *Wind Engrs. into the 21st Century: Proc., 10th Int. Conf. on Wind Engrg.*, Copenhagen, 1569–1575.

Yeh, H., and Chang, K.-T. (1994). "On propagation of edge-wave packets." *Proc., Waves—Phys. and Numer. Modeling*, M. Isaacson and M. Quick, eds., University of British Columbia, Vancouver, 270–279.

Zelt, J. A. (1986). "Tsunamis: the response of harbors with sloping boundaries to long wave excitation." *W. M. Keck Lab. Rep. No. KH-R-47*, California Institute of Technology, Pasadena, Calif.

Zhao, Z., and Fujino, Y. (1993). "Numerical simulation and experimental study of deeper-water TLD in the presence of screens." *J. Struct. Engrg.*, Tokyo, 39, 699–711.

APPENDIX II. NOTATION

The following symbols are used in this paper:

A = excitation amplitude;
C = propagation speed of uniform bore;
f_0 = resonant wave frequency in Hz based on linearized water-wave theory;
f_{b0} = resonant wave frequency for box-shaped TLD;
g = acceleration of gravity;
H = offshore incident wave height;
h = water depth ahead of uniform bore;
h_0 = water depth at rest;
L = tank bottom length;
R = runup height, i.e., vertical distance from still-water level;
s = ratio of horizontal distance over sloped surface to entire water surface;
T = excitation period;
W = length of still-water surface;
α = beach slope in radians from horizontal;
β = nondimensionalized excitation frequency;
γ = ratio of water depth of bore to water depth ahead of it;
η = water-surface elevation from still-water level;
$\bar{\eta}$ = mean water level from still-water level; and
χ = nondimensionalized resonant frequency for sloped-bottom TLD based on linearized shallow-water-wave theory.